Perlova et al. Nanoscale Research Letters (2017) 12:209
DOI 10.1186/s11671-017-1987-y

Nanoscale Research Letters

NANO COMMENTARY Open Access

Formation of Zirconium Hydrophosphate Nanoparticles and Their Effect on Sorption of Uranyl Cations

Nataliya Perlova[1*], Yuliya Dzyazko[2], Olga Perlova[1], Alexey Palchik[2] and Valentina Sazonova[1]

Abstract

Organic-inorganic ion-exchangers were obtained by incorporation of zirconium hydrophosphate into gel-like strongly acidic polymer matrix by means of precipitation from the solution of zirconium oxychloride with phosphoric acid. The approach for purposeful control of a size of the incorporated particles has been developed based on Ostwald-Freundich equation. This equation has been adapted for precipitation in ion exchange materials. Both single nanoparticles (2–20 nm) and their aggregates were found in the polymer. Regulation of salt or acid concentration allows us to decrease size of the aggregates approximately in 10 times. Smaller particles are formed in the resin, which possess lower exchange capacity. Sorption of U(VI) cations from the solution containing also hydrochloride acid was studied. Exchange capacity of the composites is ≈2 times higher in comparison with the pristine resin. The organic-inorganic sorbents show higher sorption rate despite chemical interaction of sorbed ions with functional groups of the inorganic constituent: the models of reaction of pseudo-first or pseudo-second order can be applied. In general, decreasing in size of incorporated particles provides acceleration of ion exchange. The composites can be regenerated completely, this gives a possibility of their multiple use.

Keywords: Organic-inorganic ion-exchanger, Composite, Nanoparticles, Zirconium hydrophosphate, Uranium

Background

Due to unique nuclear properties, uranium is used not only for military demands but also for civilian needs, manly as a fuel for nuclear power plants. Theoretically, about 2×10^{13} J of energy can be produced by 1 kg of uranium-235, this is an equivalent of 1.5×10^{6} kg of coal [1, 2]. Other fields of uranium application are geology and aerospace industry. Uranium is also used as a fluorescence colorant in uranium glasses.

Except traditional uranium-containing ores, such minerals as autunite [3], parsonsite [4], and monazite [5] can be a source of uranium [6], particularly deposit of monazite is located along the Sea of Azov in Ukraine [7]. Processing of monazite involves hydrochloride acid [8], in media of which uranium (VI) exists in cationic forms [9]. The problem of waste utilization arises, since the maximal permissible concentration for soluble U(VI) compounds in water is 0.015 mg dm^{-3}, but even lower values are recommended [10]. The requirements are so strict due to both radioactivity and chemical toxicity of uranium (toxicity is more dangerous than radioactivity). Uranium and decay products inflect all organs and tissues of living organisms.

In order to decrease the U(VI) content in liquid wastes down to maximal permissible concentration, chemical [11] or photocatalytic [12] reduction of soluble U(VI) compounds can be carried out. Insoluble UO_2 is formed by this manner. These methods require considerable amounts of reagents, so the problem of secondary water pollution must be solved. Similar problem is characteristic for ultrafiltration enhanced with polyelectrolytes [13]. Reverse osmosis [14] is attractive for neutral solution since the membranes, as well as ultrafiltration separators, can be damaged in acidic media.

Ion exchange and adsorption are considered as the most attractive methods for U(VI) removal from diluted solutions, particularly for tertiary treatment of water [15]. Currently, composite sorbents are considered as the most

* Correspondence: n.perlova@yandex.ua
[1]Department of Physical and Colloid Chemistry, Odessa I. I. Mechnikov National University of the MES of Ukraine, Dvoryanska str., 2, Odesa 65082, Ukraine
Full list of author information is available at the end of the article

attractive materials. They have to combine such properties as significant exchange capacity, selectivity, high rate of sorption, and facile regeneration. Additionally, the sorbents should be in a form of granules in order to provide their usage in columns. Development of the materials that possess the necessary complex of properties is the actual task.

Such composites as zirconium-antimony oxide/polyacrylonitrile [16], graphene-based materials [17–22], sorbents containing magnetic particles (iron, Fe_3O_4, and $CoFe_2O_4$) [22–27], biomaterials [28], polysulfide/layered double hydroxides [29], materials containing carbon nanotubes [25, 30], clay [31], or biopolymers [26] were proposed. Some mentioned sorbents are mechanically instable (carbon-based sorbents), some of them are destroyed in strongly acidic media during regeneration (magnetic sorbents and biomaterials). If the composite is based on inert polymer [16], its sorption capacity is insignificant. Some types of composites are suitable only for anion removal [32, 33].

Commercial strongly acidic ion-exchange resins are characterized by high sorption rate [34, 35]. However, their selectivity is low. Alternately, weakly acidic [36] or chelate [37] resins show considerable selectivity towards U(VI). At the same time, sorption on these materials is slow. In order to improve selectivity of strongly acidic resins towards Ni^{2+}, Cd^{2+}, and Pb^{2+}, they were modified with zirconium hydrophosphate (ZHP) [38–44]. The inorganic sorbent shows high selectivity towards toxic cations [45, 46], particularly U(VI) [46, 47] due to formation of complexes with functional groups [48]. Deposition of insoluble U(VI) compounds in ZHP pores is also suggested [46]. Furthermore, ZHP provides better selectivity of ion exchange membranes towards hardness ions [49]. The ion-exchanger was also applied to modification of track membrane in order to enhance its stability against fouling with organics [50].

The rate of ion exchange on the composites based on ion exchange resin depends on size of incorporated ZHP particles [38, 39, 41]. No sufficient deterioration of sorption rate was found for the composites containing non-aggregated nanoparticles [38, 39]. At the same time, particles of micron size slow down ion exchange [41]. The particle size can be controlled during the resin modification taking the Ostwald-Freundlich equation into consideration [42]. This equation was developed for precipitation from free solutions [51]. When the inorganic constituent is precipitated in ion exchange polymer, the properties of the matrix have to be considered.

Thus, the aim of the investigation is to develop the composites for removal of U(VI) cations from acidic aqueous solutions produced during monazite processing. The tasks involve adaptation of the Ostwald-Freundlich equation to modification of ion exchange matrix, experimental verification of the theoretical approach, investigation of phosphorus state in ZHP and testing of the samples.

Experimental

Modification of Ion Exchange Resin

Dowex HCR-S strongly acidic gel-like cation exchange resin (Dow Chemical) was chosen for investigations. This material, which contains ≈8% of cross-linking agent (divinylbenzene, DVB), is characterized by the highest mobility of sorbed ions among analogues [52]. A flexible gel-like resin (*Dowex WX-2*. 2% DVB) was also studied for comparison. This type of resins is usually used for electromembrane removal of divalent cations from aqueous solutions [42, 45].

The resins (polymer ion exchange matrices) were modified with amorphous ZHP. In comparison with hydrated oxides and phosphates of other metals, this material is characterized by chemical stability, particularly against hydrolysis. In opposite to crystalline modifications, amorphous ZHP can be easy regenerated.

The modification procedure involved impregnation of the resins with $ZrOCl_2$ solution followed by treatment with H_3PO_4 solution at 298 K. A ratio of volumes of solid and liquid phases was 1:100. In some cases, additionally sorbed $ZrOCl_2$ electrolyte was removed from the resin by washing with 0.01 M HCl solution before ZHP precipitation. Marking of the samples as well as the modification conditions, which were varied in opposite to [38–42], are given in Table 1.

After precipitation, the samples were washed with deionized water up to pH 7 of the effluent; dried under vacuum conditions at 343 K down to constant mass, treated with ultrasound at 30 kHz using *Bandelin* ultrasonic bath (Bandelin, Hungary), and dried in a desiccator over $CaCl_2$ at 293 K.

Determination of Grain Size and Visualization of Incorporated Particles

In each case, sizes of 300 grains were determined using Crystal-45 optical microscope (Konus, USA). The data for dominant particles are given in Table 1.

Before investigations of morphology of the composites, the samples were grinded and treated with ultrasound. *JEOL JEM 1230* transmission electron microscope (Jeol, Japan) was used for visualization of ZHP particles.

NMR Spectroscopy

The samples were inserted into the tube with a diameter of 5 mm, NMR ^{31}P spectra were measured with *AVANCE 400* spectrometer (Bruker, Germany) using single-pulse technique under the accumulation mode at 162 MHz. Chemical shift was determined relatively to 85% H_3P0_4.

Table 1 Modification of ion exchange resins with ZHP

Marking	Polymer matrix	Concentration of a $ZrOCl_2$ solution, M	Washing with a HCl solution	Concentration of a H_3PO_4 solution, M	Particle size, mm
CR-1	*Dowex HCR-S*	1.00	–	1.00	0.45
CR-2	*Dowex WX-2*	1.00	–	1.00	–
CR-3	*Dowex HCR-S*	1.00	Washing	1.00	0.31
CR-4	*Dowex HCR-S*	1.00	Washing	0.10	0.45
CR-5	*Dowex HCR-S*	1.00	Washing	0.01	0.40
CR-6	*Dowex HCR-S*	0.30	Washing	1.00	0.32
CR-7	*Dowex HCR-S*	0.10	Washing	1.00	0.39
CR-8	*Dowex HCR-S*	0.01	Washing	1.00	0.41

Sorption and Desorption of U(VI) Compounds Under Batch Conditions

The ion-exchangers based on *Dowex HCR-S* resin were applied to investigations since the resins containing 8% DVB are traditionally used for ion exchange processes. The experiments were carried out at 298 K. $UO_2Ac_2{\cdot}2H_2O$ salt (Chemapol, Czech Republic) was used for preparation of solutions. The solutions contained also HCl (0.02 M, pH 2.5), which is applied to monazite processing [8].

The solution with initial U(VI) concentration of 2×10^{-4} M was used for study of sorption rate. A series of weighted air-dry samples (0.1 g) were prepared and inserted to flasks, then deionized water was added. After swelling, water was removed and the solution (50 cm^3) was added. The content of the flasks was stirred by means of *Water Bath Shaker Type 357* (Elpan, Poland). After a predetermined time, the solid and liquid from one flask were separated; after the next period, the solution was removed from the second flask. U(VI) was determined in a form of complexes with Arsenazo III: the solution was analyzed using *Shimadzu UV-mini1240* spectrophotometer (Shimadzu, Japan) at 670 nm [53].

The degree of uranium removal (sorption degree), S, was calculated as $\frac{C_i - C_t}{C_i} \times 100\%$, where C_i and C_t are the initial concentration and concentration after certain time, respectively. Sorption capacity (A) was determined as $\frac{V(C_i - C_t)}{m}$, where V is the solution volume and m is the sorbent mass.

Exchange capacity of the samples was also determined for the solutions containing 1×10^{-5} and 1×10^{-3} M U(VI). The samples were in contact with the solutions for 24 h, the ratio of the solid and liquid is mentioned above. After sorption from the 1×10^{-3} M solution, some ion-exchangers were regenerated consequentially with deionized water, 1 M Na_2SO_4, and 1 M H_2SO_4 (the volume of each liquid was 50 cm^3). The regeneration degree was calculated as $\frac{VC}{Am}$, where C is the effluent concentration.

Results

Features of ZHP Precipitation in Ion Exchange Matrix

When precipitation of insoluble *CatAn* compound occurs in ion-exchanger, dissolution of small particles and their reprecipitation on larger particles is advantageous from a thermodynamic point of view. Gibbs energy of the system reduces due to decrease of the particle surface. The Ostwald-Freundich equation [51] reflects the effect of particle size on solubility:

$$\ln \frac{\overline{C}_{CatAn}}{C_{CatAn,\infty}} = \frac{\beta V_m \sigma}{RTr}. \quad (1)$$

Here, $\overline{C}_{CatAn}$ is the concentration of dissolved compound in the ion-exchanger, $C_{\mathrm{CatAn},\infty}$ is the concentration of saturated solution (in the case of ZHP, the $\overline{C}_{CatAn}$ and $C_{\mathrm{CatAn},\infty}$ values are extremely low), β is the shape factor of particles, V_m is the molar volume of the compound, σ is the surface tension of the solvent, R is the gas constant, r is the radius of incorporated particles.

For simplification, we can assume a charge number of one both for cations and anions. Thus, $\overline{C}_{\mathrm{CatAn}} = \left[\overline{\mathrm{Cat}^+}\right] = \frac{K_{\mathrm{sp}}}{[\mathrm{An}^-]}$, here, the square brackets correspond to equilibrium concentration, K_{sp} is the product solubility. Under excess of a precipitant containing An anions (for instance, HAn acid), it is valid:

$$[An^-] = C_{HAn} - \frac{\left[\overline{Cat^+}\right] V_i}{V_{HAn}}, \quad (2)$$

where V_i and V_{HAn} are the volumes of ion-exchanger and acid, respectively, C_{HAn} is the initial acid concentration. $\left[\overline{\mathrm{Cat}}^+\right] = A + \left[\overline{\mathrm{Cat}}^+\right]_{\mathrm{ad}}$, where A is the capacity of the ion-exchanger, $\left[\overline{\mathrm{Cat}}^+\right]_{\mathrm{ad}}$ is the concentration of additionally sorbed cations, which are present in the ion-exchanger before precipitation. Thus:

$$\overline{C}_{CatAn} = \frac{K_{sp}}{C_{HAn} - \frac{\left(A + [Cat^+]_{ad}\right)V_i}{V_{HAn}}}, \quad (3)$$

Taking formula (1) into consideration, it is possible to obtain:

$$r = \frac{V_m}{\frac{RT \ln K_{sp}}{C_{CatAn,\infty}\left(C_{HAn} - \frac{\left(A + [Cat^+]_{ad}\right)V_i}{V_{HAn}}\right)}}. \quad (4)$$

The particles of a larger size are stable thermodynamically, smaller particles are dissolved and reprecipitated.

As follows from Eq. (4), smaller particles will be formed in the resin with higher exchange capacity. Increasing in concentration of salt, which is used for impregnation of the ion-exchanger before precipitation (increase of $\left[\overline{Cat}^+\right]_{ad}$), and decreasing in acid (precipitator) concentration also cause precipitation of smaller particles inside the polymer.

Earlier the effect of molar volume of the insoluble compound on particle size has been found [54]: hydrated zirconium dioxide forms smaller particles than ZHP, which is characterized by higher V_m value. This effect is observed for precipitation in inert polymer. The influence of temperature is considered in [42].

Morphology of Ion-Exchangers

According to data of the producing company, the values of ion exchange capacity are 1.8 and 0.6 mmol cm^{-3} for *Dowex HCR-S* and *Dowex WX-2* resins, respectively. Since the $ZrOCl_2$ solution containing soluble zirconium hydroxocomplexes is strongly acidic, only a part of functional groups of the resins is involved into ion exchange during impregnation. Nevertheless, exchange capacity of *Dowex HCR-S* is expected to be higher than that for the flexible resin under these conditions. According to Eq. (4), smaller particles are formed in *Dowex HCR-S* resin (compare *CR-1* and *CR-2* samples, Fig. 1). Sizes of nanoparticles are 4–20 nm. Non-aggregated nanoparticles dominate in *CR-1*, mainly aggregates (up to 50 nm) are seen on the image for *CR-2*. Larger aggregates are formed preferably in the flexible resin evidently as a result of reprecipitation.

Porous structure of gel-like ion exchanges provides location for incorporated particles. The structure, which is formed during swelling, involves clusters (up to 20 nm) and smaller channels between them [38–42, 55–57], where functional groups are located. Larger pores (several tens and even hundreds of nanometers) are voids between gel regions. Hydrophobic fragments of hydrocarbonaceous chains are placed there. At last, pores of micron size are related to structure defects.

As shown previously [39, 40, 42], single nanoparticles are located in clusters and channels, aggregates can be placed in regions between gel fields. The particles are stabilized by pore walls, which prevent further aggregation. Formation of small aggregates is evidently caused by dissolution of nanoparticles in clusters and channels and reprecipitation in regions between gel fields. Precipitation of the inorganic constituent in pores, which exist only in swollen ion-exchanger, increase size of air-dry grains (see Table 1). The grain size of the pristine *Dowex HCR-S* resin was 0.27 mm.

Other factor determining size of incorporated particles is the amount of additionally sorbed electrolyte. The $\left[\overline{Cat}^+\right]_{ad}$ value can be controlled by washing (removal of additionally sorbed electrolyte, which was used for immersion of the ion-exchanger) on the one hand and by regulation of its initial concentration on the other hand. Figure 2 illustrates TEM images for the *CR-1*, *CR-3*, and *CR-7* samples.

The particles, size of which is larger than 1 μm, are seen in the image of the *CR-1* sample (no removal of additionally sorbed $ZrOCl_2$ during modification). Large aggregates are evidently placed in structure defects. Removal of additionally sorbed electrolyte causes a

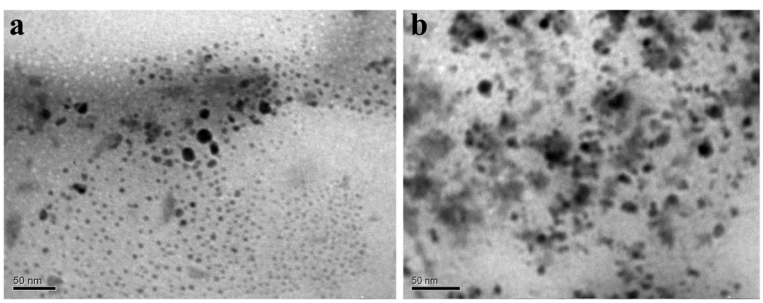

Fig. 1 ZHP nanoparticles incorporated into *Dowex HCR-S* (sample *CR-1*, **a**) and *Dowex WX-2* (sample *CR-2*, **b**)

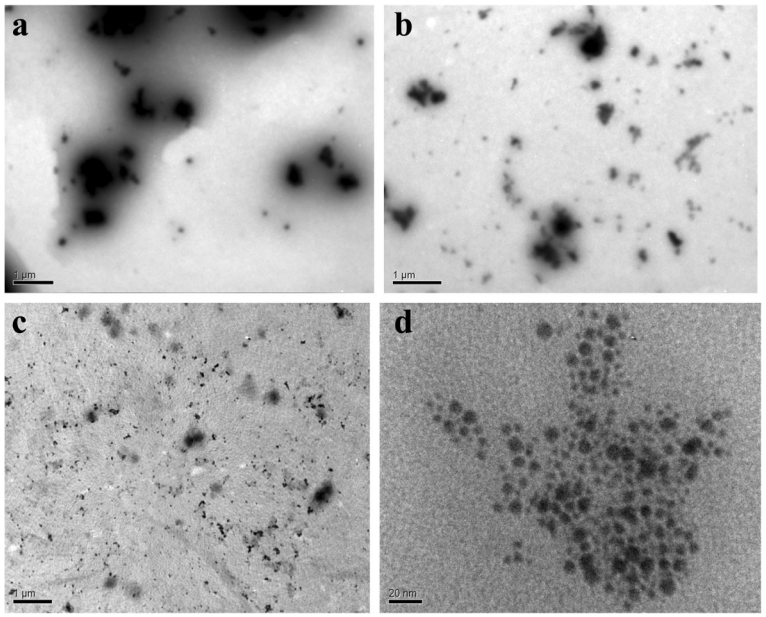

Fig. 2 TEM images of *CR-1* (**a**), *CR-3* (**b**), and *CR-7* (**c**, **d**) samples

decrease of particle size. The aggregates (up to 500 nm) are evidently located in voids between gel regions. At last, small particles (<100 nm) dominate in the *CR-7* sample, which was obtained by immersion with low concentrated $ZrOCl_2$ solution. A size of non-aggregated nanoparticles is 2–10 nm.

Decreasing in the precipitator (H_3PO_4) concentration reduces size of aggregates as seen from TEM image for the *CR-5* ion-exchanger (Fig. 3, compare with Fig. 2a). This is in accordance with Eq. (4).

State of Phosphorus in Incorporated ZHP

As shown for individual ZHP ion-exchangers, NMR ^{31}P spectra show two signals [41, 48]. It is similar also for ZHP particles in ion exchange resins [41] and membranes [58], when the inorganic constituent is in form of aggregates or agglomerates of nanoparticles [41]. These signals are attributed to hydrophosphate and dihydrophosphate groups. In the case of the samples containing non-aggregated nanoparticles, additional signals are observed (Fig. 4).

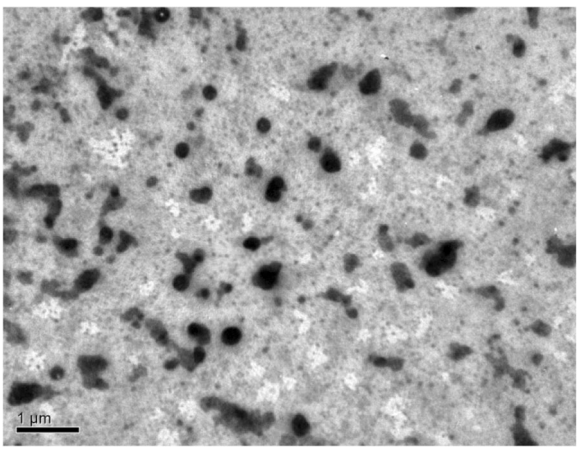

Fig. 3 TEM image of the *CR-5* ion-exchanger

The spectra are simplified with a decrease of the acid (precipitator) concentration (transition from *CR-3* to *CR-5*). Alternately, the spectra become more complex, when $ZrOCl_2$ concentration decreases (compare data for *CR-3* and *CR-6*). This is probably caused by H_3PO_4 capsulation with ZHP nanoparticles. No leaching of acid occurs during washing of the samples with deionized water. On the other hand, formation of polyphosphate in nanoreactors (clusters and channels) is possible during precipitation. Detailed analysis of the spectra is outside this work. Increase of intensity of shoulder of the signal in weak field for the CR-*3*–*CR-5* samples is observed. It means that the content of $-OPO_3H_2$ groups becomes higher.

When the acid concentration was lower than 0.3 M, no signals of phosphorus were detected (*CR-7* and *CR-8*). It means that the ZHP content is below the detection limit.

Testing of the Samples

Figure 5 illustrates degree of U(VI) sorption over time. As seen, the inorganic particles accelerate sorption (compare the data for the pristine resin and modified

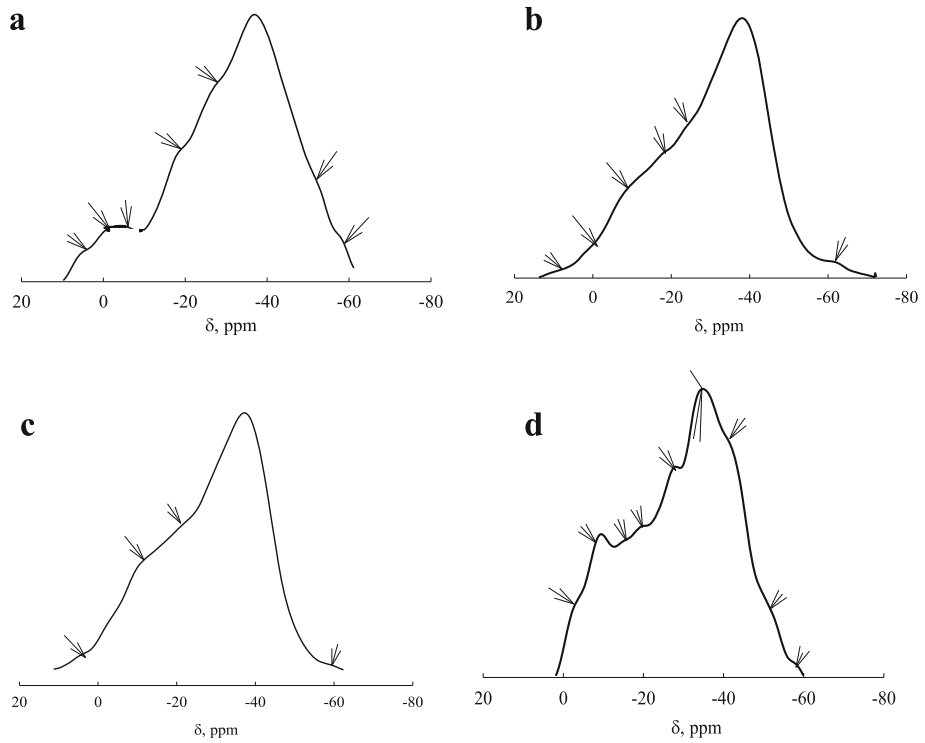

Fig. 4 NMR ^{31}P spectra for *CR-3* (**a**), *CR-4* (**b**), *CR-5* (**c**), and *CR-6* (**d**)

ion-exchangers) despite enlargement of grains after modification (see Table 1). The nanoparticles in clusters and channels screen a part of strongly acidic functional groups of the polymer matrix. Since ZHP is a weakly acidic ion-exchanger, only a part of its functional groups is involved into ion exchange. Thus, the acceleration of the process can be explained by an increase of a distance between functional groups of the polymer. Moreover, transformation of porous structure of the polymer constituent could be assumed similarly to [39–42]. However, additional investigations are needed to confirm this assumption.

Discussion

The rate of sorption decreases in the order: *CR-4* > *CR-3* > *CR-1* > *CR-5*. In general, diminution of size of the incorporated particles accelerates sorption. This tendency is also seen for other samples (*CR-6* > *CR-7* > *CR-8* > *CR-1*).

The models of film and particle diffusions [59], chemical reactions of the pseudo-first [60] and pseudo-second

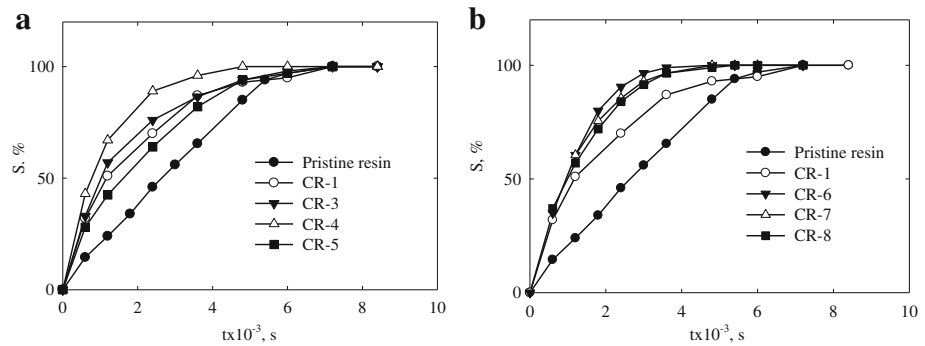

Fig. 5 Sorption of U(VI) compounds over time. Here pristine resin is *Dowex HCR-S* (**a**, **b**). Other samples are: *CR-1* (**a**, **b**), *CR-3*, *CR-4*, *CR-5* (**a**), *CR-6*, *CR-7*, *CR-8* (**b**)

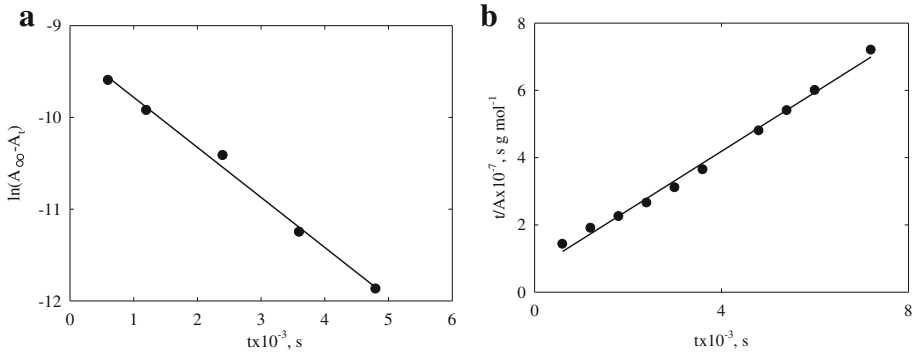

Fig. 6 Models of chemical reaction of pseudo-first (**a**) and pseudo-second order (**b**) applied to U(VI) sorption on the *CR-1* and *CR-6* samples

order [61] were used. As found, the *CR-1* and *CR-3*–*CR-5* composites obey the model of the pseudo-first order:

$$\ln (A_\infty - A_t) = \ln A_\infty - K_1 t. \quad (5)$$

At the same time, the model of the pseudo-second order

$$\frac{t}{A} = \frac{1}{K_2 A_\infty^2} + \frac{1}{A_\infty} \cdot t. \quad (6)$$

can be applied to *CR-6*-*CR-8* samples. Here, A_t and A_∞ are the capacity after certain time and under equilibrium conditions, respectively, K_1 and K_2 are the constants. The results for some samples are given in Fig. 6, the data are summarized in Tables 2 and 3.

Thus, sorption rate is determined by size of incorporated ZHP particles on the one hand and by interaction of sorbed UO_2^{2+} ions with functional groups of the inorganic constituent on the other hand. If the interaction is complex formation similarly to [48], mainly $-(O)_2PO_2H$ groups are involved to sorption (*CR-1*, *CR-3*, *CR-4*, and *CR-5*). When ZHP is precipitated with considerable excess of H_3PO_4, significant amount of $-OPO_3H_2$ groups is formed (compare Fig. 4a and d). In this case, UO_2^{2+} ions interact with them, since these groups are more acidic. However, deposition of insoluble U(VI) compounds is also possible [46]. Detailed investigation of sorption mechanism is a task of future investigations.

Sorption capacity, which is reached in solutions of various concentrations, is given in Table 4 for some samples. Comparing with the pristine resin, the ion-exchangers are characterized by higher exchange capacity. The highest A_∞ values for less and more concentrated solutions were found for the sample containing small aggregates (*CR-7*). In opposite to the sample containing particles of micron size, lower amount of aggressive reagent (H_2SO_4) is necessary for regeneration.

Conclusions

A size of ZHP particles incorporated into ion-exchange polymers can be controlled during modification procedure by regulation of concentration of $ZrOCl_2$ and H_3PO_4 solutions as well as by removal of additionally sorbed $ZrOCl_2$. Decrease of the concentration allows us to obtain small particles (both non-aggregated nanoparticles and their aggregates) and avoid formation of agglomerates of micron size. Complex structure of NMR ^{31}P spectra has been found. This can be caused by H_3PO_4 capsulation in clusters and channels of the polymer on the one hand and by polyphosphate formation on the other hand.

Testing of the samples shows faster sorption of U(VI) cations on the modified sample comparing with the pristine resin. The exchange is complicated by chemical interaction of sorbed U(VI) ions with functional groups of ZHP: the rate of exchange is described by the models of chemical reaction of the pseudo-first or pseudo-second order. Thus, selectivity of the composites towards U(VI) ions is expected for the solution

Table 2 Models of chemical reaction of the pseudo-first order

Sample	$A_\infty \times 10^4$, mol g^{-1}		$K_1 \times 10^4$, s^{-1}	R^2
	Experimental	Calculated from Eq. (5)		
CR-1	1.00	0.95	5.0	0.993
CR-3	1.00	0.97	5.1	0.991
CR-4	1.00	0.95	8.9	0.999
CR-5	1.00	1.07	5.1	0.995

Table 3 Models of chemical reaction of the pseudo-second order

Sample	$A_\infty \times 10^4$, mol g^{-1}		K_2, g mol^{-1}s^{-1}	R^2
	Experimental	Calculated from Eq. (6)		
CR-6	1.00	1.17	9.02	0.985
CR-7	1.00	1.19	7.94	0.990
CR-8	1.00	1.19	7.47	0.992

Table 4 Sorption capacity towards U(VI) and regeneration of the samples

Sample	$A_\infty \times 10^4$, mol g^{-1}		Regeneration degree, %			
	$C_i = 1 \times 10^{-5}$ M	$C_i = 1 \times 10^{-3}$ M	Water	Na_2SO_4	H_2SO_4	Total
Pristine resin	0.042	4.00	2	60	38	100
CR-3	0.099	3.95	2	15	83	100
CR-7	0.098	5.07	2	24	74	100

containing other inorganic ions. The sorbents can be used in acidic media.

Control of particle size by regulation of salt concentration looks preferably since ZHP obtained by this manner accelerates sorption despite initial $ZrOCl_2$ content in the resin before precipitation. The ion-exchanger obtained by this manner shows significant exchange capacity in wide interval of U(VI) concentration. The approach developed in this work could be used further for purposeful control of particle size in ion exchange polymers.

Acknowledgements
The work was supported by projects within the framework of programs supported by the National Academy of Science of Ukraine "Fundamental problems of creation of new materials for chemical industry" (grant no. 49/12).

Authors' Contributions
NP carried out sorption experiments and drafted the manuscript. YD performed development of theoretical approach and characterization of the materials. OP provided chemical analysis and modeling of sorption. AP synthesized organic-inorganic ion-exchangers. VS contributed to the valuable discussions on experimental and theoretical results. All authors read and approved the final manuscript.

Competing Interests
The authors declare that they have no competing interests.

Publisher's Note

Author details
[1]Department of Physical and Colloid Chemistry, Odessa I. I. Mechnikov National University of the MES of Ukraine, Dvoryanska str., 2, Odesa 65082, Ukraine. [2]Department of Sorption and Membrane Materials and Processes, V.I. Vernadskii Institute of General and Inorganic Chemistry of the NAS of Ukraine, Palladin ave. 32/34, Kyiv 03142, Ukraine.

Received: 29 December 2016 Accepted: 9 March 2017
Published online: 21 March 2017

References

1. Emsley J (2001) Uranium. In: Nature's building blocks: an A to Z guide to the elements. Oxford University Press, Oxford, pp 476–482
2. Uranium Processing and Properties. Morrell JS, Jackson MJ, editors. New York, Heidelberg, Dordrecht: Springer; 2013
3. Edwards CR, Oliver AJ (2000) Uranium processing: a review of current methods and technology. JOM 52(9):12–20
4. Anvia M, Brown SA, McOrist GD (2015) The deportment of uranium decay chain radionuclides during processing of an Australian monazite concentrate using a caustic conversion route. J Radioanal Nucl Chem 303(2):1393–1398
5. Korzeb SL, Foord EE, Lichte FE (1997) The chemical evolution and paragenesis of uranium minerals from the ruggles and palermo granitic pegmatites, New Hampshire. Can Mineral 35:135–144
6. Uranium Prospecting Handbook: Proceedings of a NATO Sponsored Advanced Study Institute on Methods of Prospecting for Uranium Minerals. Bowie SHU, Davis M, Ostle D, editors. London: Institution of Mining and Metallurgy; 1972
7. Dumańska-Słowik M, Budzyń B, Heflik W, Sikorska M (2012) Stability relationships of REE-bearing phosphates in an alkali-rich system (nepheline syenite from the Mariupol Massif, SE Ukraine). Acta Geol Pol 62(2):247–265
8. Kumari A, Panda P, Jha MK, Lee JY, Kumar JR, Kumar V (2015) Thermal treatment for the separation of phosphate and recovery of rare earth metals (REMs) from Korean monazite. J Ind Eng Chem 21: 696–703
9. Gapel G (2005) Speciation of actinides. In: Cormelis R, Caruso JA, Crews H, Heumann KG (eds) Handbook of elemental speciation II. Species in the environment, food, medicine and occupational health. Wile, Chichester, pp 509–563
10. Brine W (2010) The toxicity of depleted uranium. Int J Environ Res Public Health 7(1):303–313
11. Hua B, Xu H, Terry J, Deng B (2006) Kinetics of uranium(VI) reduction by hydrogen sulfide in anoxic aqueous systems. Environ Sci Technol 40(15): 4666–4671
12. Sandhu SS, Kohli KB, Brar AS (1984) Photochemical reduction of the uranyl ion with dialkyl sulfides. Inorg Chem 23(22):3609–3612
13. Roach JD, Zapien JH (2009) Inorganic ligand-modified, colloid-enhanced ultrafiltration: a novel method for removing uranium from aqueous solution. Water Res 43(18):4751–4759
14. Montaña M, Camacho A, Serrano I, Devesa R, Matia L, Vallés I (2013) Removal of radionuclides in drinking water by membrane treatment using ultrafiltration, reverse osmosis and electrodialysis reversal. J Environ Radioact 125:86–92
15. Kim J, Tsouris C, Mayes RT, Oyola Y, Saito T, Janke CJ, Dai S et al (2013) Recovery of uranium from seawater: a review of current status and future research needs. Sep Sci Technol 48(3):367–387
16. Cakir P, Inan S, Altas Y (2014) Investigation of strontium and uranium sorption onto zirconium-antimony oxide/polyacrylonitrile (Zr-Sb oxide/PAN) composite using experimental design. J Hazard Mater 271:108–119
17. Li ZJ, Wang L, Yuan LY, Xiao CL, Mei L, Zheng LR et al (2015) Efficient removal of uranium from aqueous solution by zero-valent iron nanoparticle and its graphene composite. J Hazard Mater 290:26–33
18. Shao D, Hou G, Li J, Wen T, Ren X, Wang X (2014) PANI/GO as a super adsorbent for the selective adsorption of uranium (VI). Chem Eng J 255: 604–612
19. Shao DD, Li JX, Wang XK (2014) Poly (amidoxime)-reduced graphene oxide composites as adsorbents for the enrichment of uranium from seawater. Sci China Chem 57(11):1449–1458
20. Cheng H, Zeng K, Yu J (2013) Adsorption of uranium from aqueous solution by graphene oxide nanosheets supported on sepiolite. J Radioanal Nucl Chem 298(1):599–603
21. Tan L, Wang Y, Liu Q, Wang J, Jing X, Liu L et al (2015) Enhanced adsorption of uranium (VI) using a three-dimensional layered double hydroxide/graphene hybrid material. Chem Eng J 259:752–760
22. Sun YB, Ding CC, Cheng WC, Wang XK (2014) Simultaneous adsorption and reduction of U (VI) on reduced graphene oxide-supported nanoscale zerovalent iron. J Hazard Mater 280:399–408
23. Fan FL, Qin Z, Bai J, Rong WD, Fan FY, Tian W et al (2012) Rapid removal of uranium from aqueous solutions using magnetic Fe3O4@SiO2 composite particles. J Environ Radioact 106:40–46
24. Tan L, Zhang X, Liu Q, Jing X, Liu J, Song D et al (2015) Synthesis of Fe3O4-TiO2 core–shell magnetic composites for highly efficient

sorption of uranium (VI). Colloids Surf A Physiochem Eng Asp 469:279–286
25. Tan L, Liu Q, Jing X, Liu J, Song D, Hu S et al (2015) Removal of uranium (VI) ions from aqueous solution by magnetic cobalt ferrite/multiwalled carbon nanotubes composites. Chem Eng J 273:307–315
26. Hritcu D, Humelnicu D, Dodi G, Popa MI (2012) Magnetic chitosan composite particles: evaluation of thorium and uranyl ion adsorption from aqueous solutions. Carbohydr Polym 87(2):1185–1191
27. Zhao Y, Li J, Zhao L, Zhang S, Huang Y, Wu X, Wang X (2014) Synthesis of amidoxime-functionalized Fe_3O_4@SiO_2 core–shell magnetic microspheres for highly efficient sorption of U(VI). Chem Eng J 235:275–283
28. Akhtar K, Khalid AM, Akhtar MW, Ghaur MA (2009) Removal and recovery of uranium from aqueous solutions by Ca-alginate immobilized Trichoderma harzianum. Bioresour Technol 100(20):4551–4558
29. Ma S, Huang L, Ma L, Shim Y, Islam SM, Wang P et al (2015) Efficient uranium capture by polysulfide/layered double hydroxide composites. J Am Chem Soc 137(10):3670–3677
30. Abdeen Z, Akl ZF (2015) Uranium (VI) adsorption from aqueous solutions using poly(vinyl alcohol)/carbon nanotube composites. RSC Adv 5:74220–74229
31. Yu HW, Yang SS, Ruan HM, Shen JN, Gao CJ, Van der Bruggen B (2015) Recovery of uranium ions from simulated seawater with palygorskite/amidoxime polyacrylonitrile composite. Appl Clay Sci 111:67–75
32. Yaroshenko NA, Sazonova VF, Perlova OV, Perlova NA (2012) Sorption of uranium compounds by zirconium-silica nanosorbents. Russ J Appl Chem 85(6):849–855
33. Perlova OV, Sazonova VF, Perlova NA, Yaroshenko NA (2014) Kinetics of sorption of uranium(VI) compounds with zirconium-silica nanosorbents. Russ J Phys Chem A 88(6):1012–1016
34. Kilislioglu A, Bilgin B (2003) Thermodynamic and kinetic investigations of uranium adsorption on amberlite IR-118H resin. Appl Radiat Isot 58(2):155–160
35. Korkisch J, Ahluwalia SS (1966) Separation of uranium by combined ion exchange-solvent extraction. Anal Chem J 38(3):497–500
36. Dabrowski A, Hubicki Z, Podkościelny P, Robens E (2004) Selective removal of the heavy metal ions from waters and industrial wastewaters by ion-exchange method. Chemosphere 56(2):91–106
37. Chiarizia R, Horwitz EP, Alexandratos SD (1994) Uptake of metal ions by a new chelating ion-exchange resin. Part 4: kinetics. Solvent Extr Ion Exch 12(1):211–237
38. Dzyazko YS, Ponomareva LN, Volfkovich YM, Sosenkin VE (2012) Effect of the porous structure of polymer on the kinetics of Ni^{2+} exchange on hybrid inorganic-organic ionites. Russ J Phys Chem A 86(6):913–919
39. Dzyazko YS, Ponomaryova LN, Volfkovich YM, Sosenkin VE, Belyakov VN (2013) Polymer ion-exchangers modified with zirconium hydrophosphate for removal of Cd^{2+} ions from diluted solutions. Separ Sci Technol 48(14): 2140–2149
40. Dzyazko YS, Ponomareva LN, Volfkovich YM, Sosenkin VE, Belyakov VN (2013) Conducting properties of a gel ionite modified with zirconium hydrophosphate nanoparticles. Russ J Electrochem 49(3):209–215
41. Dzyazko YS, Ponomaryova LN, Volfkovich YM, Trachevskii VV, Palchik AV (2014) Ion-exchange resin modified with aggregated nanoparticles of zirconium hydrophosphate. Morphology and functional properties. Microporous Mesoporous Mater 198:55–62
42. Dzyazko YS, Volfkovich YM, Ponomaryova LN, Sosenkin VE, Trachevskii VV, Belyakov VN (2016) Composite ion-exchangers based on flexible resin containing zirconium hydrophosphate for electromembrane separation. J Nanosci Technol 2:43–49
43. Pan BC, Zhang QR, Zhang WM, Pan BJ, Du W, Lu L et al (2007) Highly effective removal of heavy metals by polymer-based zirconium phosphate: a case study of lead ion. J Colloid Interface Sci 310:99–105
44. Zhang Q, Pan B, Zhang S, Wang J, Zhang W, Lu L (2011) New insights into nanocomposite adsorbents for water treatment: a case study of polystyrene-supported zirconium phosphate nanoparticles for lead removal. J Nanopart Res 13:5355–5364
45. Dzyaz'ko YS, Rozhdestvenskaya LM, Palchik AV (2005) Recovery of nickel ions from dilute solutions by electrodialysis combined with ion exchange. Russ J Appl Chem 75(3):414–421
46. Zakutevskyy OI, Psareva TS, Strelko VV (2012) Sorption of U(VI) ions on sol-gel-synthesized amorphous spherically granulated titanium phosphates. Russ J Appl Chem 85(9):1366–1370
47. Zhuravlev I, Zakutevsky O, Psareva T, Kanibolotsky V, Strelko V, Taffet M, Gallios G (2002) Uranium sorption on amorphous titanium and zirconium phosphates modified by Al^{3+} or Fe^{3+} ions. J Radioanal Nucl Chem 254(1):85–89
48. Dzyazko YS, Trachevskii VV, Rozhdestvenskaya LM, Vasilyuk SL, Belyakov VN (2013) Interaction of sorbed Ni(II) ions with amorphous zirconium hydrogen phosphate. Russ J Phys Chem A 87(5):840–845
49. Dzyazko Y, Rozhdestveskaya L, Zmievskii Y, Volfkovich Y, Sosenkin V, Nikolskaya N et al (2015) Heterogeneous membranes modified with nanoparticles of inorganic ion-exchangers for whey demineralization. Mater Today: Proceedings 2(6):3864–3873
50. Dzyazko YS, Rozhdestvenskaya LM, Zmievskii YG, Vilenskii AI, Myronchuk VG, Kornienko LV et al (2015) Organic-inorganic materials containing nanoparticles of zirconium hydrophosphate for baromembrane separation. Nanoscale Res Lett 10:64
51. Myerson AS (2002) Handbook of Industrial Crystallization. Butterworth-Heinemann, Boston
52. Dzyazko YS, Belyakov VN (2004) Purification of a diluted nickel solution containing nickel by a process combining ion exchange and electrodialysis. Desalination 162:179–189
53. Kadam BV, Maiti B, Sathe RM (1981) Selective spectrophotometric method for the determination of uranium(VI). Analyst 106:724–726
54. Myronchuk VG, Dzyazko YS, Zmievskii YG, Ukrainets AI, Bildukevich AV, Kornienko LV et al (2016) Organic-inorganic membranes for filtration of corn distillery. Acta Periodica Technologica 47:153–165
55. Berezina NP, Vol'fkovich YM, Kononenko NA, Blinov IA (1987) Water distribution studies in heterogeneous ion-exchange membranes by standard porosimetry. Soviet Electrochem 23:858–862
56. Hsu WY, Gierke TD (1983) Ion transport and clustering in Nafion perfluorinated membranes. J Membr Sci 13(3):307–326
57. Yaroslavtsev AB, Nikonenko VV (2009) Ion-exchange membrane materials: properties, modification, and practical application. Nanotechnol in Russia 4(3):137–159
58. Nicotera I, Khalfan A, Goenaga G, Zhang T, Bocarsly A, Greenbaum S (2008) NMR investigation of water and methanol mobility in nanocomposite fuel cell membranes. Ionics 14(3):243–253
59. Helfferich F (1995) Ion exchange. Dover, New York
60. Lagergren S (1898) About the theory of so called adsorption of soluble substances. Kungliga Svenska Vetenskapsakademiens Handlingar 24(4):1–39
61. Ho YS, McKay G (1999) Pseudo-second order model for sorption processes. Process Biochem 34(5):451–465